August 17th, 2026

EMC Modeling and Low-Band EMI Filter Design for Grid-to-Truck Electric Powertrain System Using MATLAB/Simulink

Palaniappan Sakthivel and Emmanuel A Peter

MASTER THESIS
Electromechanical Vehicle Engineering
Department of Engineering Science

August 17th, 2026

MASTER THESIS

EMC Modeling and Low-Band EMI Filter Design for Grid-to-Truck Electric Powertrain System Using MATLAB/Simulink

Abstract

This thesis investigates low-band conducted EMI in a grid-to-truck electric powertrain and evaluates a passive EMI filter using MATLAB/Simulink. The study focuses on the effect of converter switching on the voltage and current frequency spectra and the reduction of switching-related components through passive filtering. A simulation model was developed that includes the main parts of the electric powertrain, such as the DC-link, machine-side converter, field-oriented control system, three-phase electrical network, asynchronous machine, and mechanical load. A three-stage passive EMI filter was placed between the converter and the machine. The filter consists of a three-phase series inductive stage, a three-winding coupled inductor, and a three-phase RC stage. The voltage and current signals were then studied in the frequency domain over a range of 0–20 kHz.

The results without the filter showed clear frequency components around the 2 kHz PWM switching frequency and its multiples, particularly around 4, 6, 8, and 10 kHz. After the filter was introduced, these switching-related components were noticeably reduced. At selected frequencies between 2 and 10 kHz, reductions of approximately 17–28 dB were observed, while the higher-frequency region also generally showed lower spectral levels. This shows that the proposed filter can reduce unwanted switching-related frequency components within the simulated powertrain system.

The results are mainly used to compare the system before and after filtering under the same simulation conditions. Since the investigated frequency range of 0–20 kHz is below the conventional CISPR 25 conducted-emission measurement range, the results cannot be used to demonstrate EMC compliance. Overall, the study shows that MATLAB/Simulink can be useful for studying low-band conducted EMI and evaluating passive filtering approaches before moving to experimental testing.

Date:	August 17, 2026
Author(s):	Palaniappan Sakthivel, Emmanuel Adesi Peter
Examiner:	Mikael Alatalo (University West)
Advisor(s):	Michelle Hunt
Programme name:	Electromechanical Vehicle Engineering
Main field of study:	Engineering
Course credits:	15 HE credits
Publisher:	University West, Department of Engineering Science, S-461 86 Trollhättan, SWEDEN

Contents

1 Introduction 1
1.1 Background ... 1
1.1.1 Grid-to-Truck Powertrain and Pantograph Connection ... 2
1.2 Aim of the Study ... 2
1.3 Problem Definition ... 3
1.4 Limitations ... 4

2 THEORY 4
2.1 SOURCES OF EMI/EMC NOISE IN ELECTRIFIED POWERTRAIN ... 4
2.1.1 COMMON MODE (CM) AND DIFFERENTIAL MODE (DM) NOISE ... 4
2.1.2 COMMON MODE CONDUCTED AND RADIATED EMISSION ... 6
2.2 DESIGN OF THE FILTER ... 7
2.2.1 DESIGN CONFIGURATION OF THE PASSIVE STAGE FILTER ... 7
2.3 CONDUCTED ELECTROMAGNETIC INTERFERENCE ... 8
2.4 Y-Capacitor FOR Common-mode Noise Mitigation ... 9
2.5 EMC STANDARDS RELATED TO ELECTRIC VEHICLE POWERTRAINS ... 9
2.5.1 ELECTRIC VEHICLE EMISSION FREQUENCY RANGE ... 10

3 METHOD 11
3.1 Methodology ... 11
3.2 Model Reduction and Scope of the Simulation ... 11
3.3 System Design And Simulation ... 12
3.3.1 DC-Link Supply ... 12
3.3.2 Machine Side Converter ... 12
3.3.3 Field Oriented Control System ... 13
3.3.4 Voltage and Current Measurement Subsystem ... 13
3.3.5 Three Phase Series Inductor / Low-Pass Filter Stage ... 14
3.3.6 Three Winding Mutual Inductor ... 14
3.3.7 Three Phase RC Filter Stage ... 14
3.3.8 Asynchronous Machine ... 15
3.3.9 Mechanical Load and Torque Subsystem ... 15
3.4 Presentation of Results Based on Model and Simulation ... 15
3.4.1 Final Simulation Model with Filter ... 15

4 RESULTS 18
4.1 CONDUCTED EMI ANALYSIS ... 18
4.1.1 EMI SPECTRUM ANALYSIS WITHOUT FILTER ... 18
4.1.2 EMI SPECTRUM ANALYSIS WITH FILTER ... 20
4.1.3 Performance Assessment of the EMC ... 23

5 Discussion of Results 24
5.1 Comparison with EMC Standards ... 25

6 CONCLUSION 26
6.1 Limitations of the Work ... 27
6.2 Recommendation for Future Work ... 28

Figures

Figure 1. Differential Mode noise and Common Mode noise in EV Propulsion System.
Figure 2. Differential Mode noise and Common Mode noise area in EV System
Figure 3. Basic components of Passive Stage Filters
Figure 4. Simplified circuit model of the Y-capacitor
Figure 5. Final Simulation Model with Filter
Figure 6. Conducted EMI Voltage Spectrum without EMI Filter
Figure 7. Conducted EMI Current Spectrum without EMI Filter
Figure 8. Conducted EMI Voltage Spectrum with EMI Filter
Figure 9. Conducted EMI Current Spectrum with EMI Filter

Tables

Table 1. Simulink Configuration Parameters
Table 2. Power levels comparison before and after filtering

1 Introduction

The following chapter will consist of the information for the introduction of the project, with the clear and concise description of the background, the aim of the project, its limitations and problems.

1.1 Background

The worldwide shift towards sustainable transportation has expedited the implementation of electric vehicles (EVs), especially in the heavy-duty transportation industry. Electric trucks are progressively being engineered to diminish greenhouse gas emissions, enhance energy efficiency, and advance environmental sustainability objectives according to [1]. The expansion of electrified transportation systems has led to an increased prominence of high-power electronic converters and sophisticated control systems in electric powertrains. While these technologies enhance vehicle efficiency and performance, they also present considerable electromagnetic compatibility (EMC) concerns as stated by [2]. Electric powertrain systems depend significantly on high-speed switching power electronic components, such Insulated Gate Bipolar Transistors (IGBTs) and Metal-Oxide Semiconductor Field-Effect Transistors (MOSFETs). These devices produce high-frequency switching transients marked by elevated rates of voltage change (dv/dt) and current change (di/dt). Consequently, undesirable electromagnetic interference (EMI) is generated within the system [3]. Electromagnetic interference (EMI) can traverse conductive pathways, radiated fields, and parasitic coupling mechanisms, possibly impacting adjacent electronic devices and communication networks. In grid-to-truck electric powertrain systems, conducted electromagnetic interference (EMI) is particularly concerning due to the direct electrical linkage among the charging infrastructure, power converters, and vehicle systems. Excessive electromagnetic interference may disrupt vehicle control units, communication buses, sensors, and safety-critical electronics, resulting in diminished system reliability and performance [3].

The worldwide shift towards sustainable transportation has expedited the implementation of electric vehicles (EVs), especially in the heavy-duty transportation industry. Electric trucks are progressively being engineered to diminish greenhouse gas emissions, enhance energy efficiency, and advance environmental sustainability objectives [1]. The expansion of electrified transportation systems has led to an increased prominence of high-power electronic converters and sophisticated control systems in electric powertrains. While these technologies enhance vehicle efficiency and performance, they also present considerable electromagnetic compatibility (EMC) concerns [2]. Electric powertrain systems depend significantly on high-speed switching power electronic components, such Insulated Gate Bipolar Transistors (IGBTs) and Metal-Oxide Semiconductor Field-Effect Transistors (MOSFETs). These devices produce high-frequency switching transients marked by elevated rates of voltage change (dv/dt) and current change (di/dt). Consequently, undesirable electromagnetic interference (EMI) is generated within the system [3]. Electromagnetic interference (EMI) can traverse conductive pathways, radiated fields, and parasitic coupling mechanisms, possibly impacting adjacent electronic devices and communication networks. In grid-to-truck electric powertrain systems, conducted electromagnetic interference (EMI) is particularly concerning due to the direct electrical linkage among the charging infrastructure, power converters, and vehicle systems. Excessive electromagnetic interference may disrupt vehicle control units, communication buses, sensors, and safety-critical electronics, resulting in diminished system reliability and performance [3].

Furthermore, according to [6] and [7] electric vehicles are required to comply with strict EMC standards and automotive regulations to ensure safe and reliable operation in real-world environments, such as CISPR 25 and ISO 11452 standards.
An EMI problem generally consists of three main elements: the source, the coupling path, and the victim. The source refers to the electronic component generating electromagnetic noise, such as the machine-side converter or switching inverter. The coupling path, often influenced by parasitic capacitances and inductances, represents the medium through which the interference propagates. The victim refers to sensitive electronic equipment affected by the noise. [1] and [2] reiterates that the effective EMC design aims to minimize EMI by reducing noise generation, interrupting coupling paths, or improving the immunity of sensitive systems.
To address these challenges, EMI filters are widely employed in electric powertrain systems to suppress unwanted conducted emissions. Low-band EMI filters are particularly important for reducing low-frequency conducted noise generated by switching converters and power electronics [9]. Proper filter design requires accurate system modeling and simulation to predict EMI behavior and optimize filter performance before hardware implementation.
MATLAB/Simulink provides a powerful platform for modeling and analyzing EMC behavior in electric powertrain systems. Through simulation, it is possible to evaluate switching characteristics, parasitic effects, cable interactions, and conducted emission levels under various operating conditions [5]. Simulation-based approaches also reduce development cost and design time by enabling early-stage EMC assessment and filter optimization.

1.1.1 Grid-to-Truck Powertrain and Pantograph Connection

In the investigated grid-to-truck application, the vehicle receives electrical power from the external grid through a pantograph. Unlike a conventional battery-electric vehicle, where the main energy source is an onboard battery, a grid-to-truck vehicle can remain connected to the external power supply while driving. The electrical power from the pantograph is supplied to the vehicle's power electronics, including the DC-link and motor controller, which then provide the required power to the traction motor.
This continuous connection between the vehicle and the electrical grid also creates an important EMC concern. The switching operation of the motor controller can generate electrical disturbances that may propagate through the vehicle's electrical system and potentially reach the grid-side infrastructure. Therefore, reducing these switching-related conducted disturbances is important for improving the EMC behavior of the overall system.
In this thesis, the complete grid-to-truck system is represented using a simplified simulation model. The pantograph and grid-side connection provide the application context, while the detailed investigation focuses on the DC-link, machine-side converter, filter network, and traction motor. This simplified approach makes it possible to study the switching-related disturbances and investigate how the proposed low-pass filter can reduce these disturbances.

1.2 Aim of the Study

The aim of this thesis is to investigate electromagnetic compatibility (EMC) challenges in grid-to-truck electric powertrain systems and to develop an effective low-band electromagnetic interference (EMI) filter design using MATLAB/Simulink simulation tools.

With the increasing adoption of electric vehicles, particularly in heavy-duty transportation applications, the integration of high-power electronic converters and fast-switching semiconductor devices has significantly increased the generation of conducted and radiated electromagnetic emissions within electric powertrain systems as stated by [2]. These emissions can negatively affect the operation of sensitive electronic components, communication networks, sensors, and safety-critical vehicle systems, thereby making EMC an essential consideration in modern electric vehicle design [3].

This study specifically focuses on using MATLAB/Simulink to model the electromagnetic behavior of a grid-to-truck electric powertrain system to identify and analyze major EMI sources such as machine-side converters, DC-link components, switching devices, and parasitic coupling elements. The research investigates how high-frequency switching operations and parasitic effects contribute to conducted EMI propagation within the system. By developing a detailed simulation model in MATLAB/Simulink, the study aims to provide a better understanding of EMI generation mechanisms on Grid-to-Truck Electric power train system.

One of the major challenges in EMI mitigation is the accurate modeling of EMI generation and propagation mechanisms within complex electric powertrain systems. Parasitic capacitances, inductances, cable interactions, grounding configurations, and switching characteristics significantly influence EMI behavior, making EMC analysis difficult during the design stage according to [8]. Without proper modeling and filtering techniques, unwanted emissions may only become visible during hardware testing, resulting in increased development cost, redesign efforts, and delays in product implementation.

Therefore, there is a need for an effective simulation-based approach to model electromagnetic behavior and develop suitable low-band EMI filters capable of reducing conducted emissions in grid-to-truck electric powertrain systems. This study addresses this challenge by using MATLAB/Simulink to investigate EMI sources, analyze conducted emission characteristics, and design a low-band EMI filtering solution that improves electromagnetic compatibility and supports compliance with automotive EMC requirements.

1.3 Problem Definition

In grid-to-truck electric powertrain systems, conducted EMI presents a major EMC concern because of the direct electrical interaction between the grid infrastructure, charging systems, and vehicle power electronics as noted from [3] and [4]. Excessive EMI may interfere with sensitive electronic control units (ECUs), communication buses, sensors, and monitoring systems, potentially leading to signal distortion, communication errors, degraded system performance, or malfunction of safety-critical components [2]. Furthermore, failure to comply with automotive EMC standards such as CISPR 25 and ISO 11452 can limit system reliability, certification, and commercial deployment [6] and [7].

One of the major challenges in EMI mitigation is the accurate modeling of EMI generation and propagation mechanisms within complex electric powertrain systems. Parasitic capacitances, inductances, cable interactions, grounding configurations, and switching characteristics significantly influence EMI behavior, making EMC analysis difficult during the design stage [8]. Without proper modeling and filtering techniques, unwanted emissions may only become visible during hardware testing, resulting in increased development cost, redesign efforts, and delays in product implementation.

1.4 Limitations

This study focuses primarily on conducted electromagnetic interference (EMI) within grid-to-truck electric powertrain systems and does not provide an extensive investigation of radiated EMI phenomena. The research is limited to low-band EMI filter design and analysis, with greater emphasis placed on low-frequency conducted emissions generated by switching power electronic devices.

The study is based mainly on simulation modeling using MATLAB/Simulink; therefore, the accuracy of the results depends on the assumptions, parameters, and simplifications used in the simulation environment by [5]. Certain real-world factors such as environmental noise, manufacturing tolerances, temperature variations, aging effects, and complex electromagnetic interactions may not be fully represented within the simulation models.

In addition, the research considers selected EMI sources within the electric powertrain system, including the machine-side converter, DC-link components, and switching devices. Other possible EMI contributors, such as auxiliary vehicle systems, wireless communication modules, and external electromagnetic disturbances, are outside the scope of this study.

The filter design developed in this thesis is intended specifically for the modeled grid-to-truck electric powertrain configuration and may require further optimization or modification for application in different vehicle architectures, power ratings, or charging infrastructures. Furthermore, the study focuses on simulation-based EMC analysis and does not include full-scale experimental hardware validation due to time, equipment, and resource constraints.

Despite these limitations, the study provides valuable insight into EMC modeling and low-band EMI filter design for electric powertrain systems and establishes a foundation for future experimental validation and advanced EMC optimization research as per [8] and [9].

2 THEORY

This chapter presents the theoretical foundations relevant to electromagnetic compatibility (EMC) modeling and low-band electromagnetic interference (EMI) filter design in grid-to-truck electric powertrain systems. The increasing integration of high-power electronic converters and fast-switching semiconductor devices in electric vehicles (EVs) has led to significant EMI challenges, making EMC a critical design requirement.

This chapter discusses the fundamental concepts of EMC and EMI, EMI generation in power electronic systems, EMI propagation mechanisms, conducted EMI characteristics, and the principles of EMI filter design. Emphasis is placed on low-band conducted EMI and its mitigation using passive filtering techniques. These theoretical concepts form the basis for the modeling and simulation work presented in subsequent chapters.

2.1 SOURCES OF EMI/EMC NOISE IN ELECTRIFIED POWERTRAIN

2.1.1 COMMON MODE (CM) AND DIFFERENTIAL MODE (DM) NOISE

Electric propulsion systems, particularly traction inverters and motor drives, are significant sources of electromagnetic noise within electric vehicles. These noise currents propagate through high-voltage cables and busbars before returning to the power or signal source. A typical high-voltage propulsion architecture consists of a three-phase inverter connected to an AC traction motor, as illustrated in Fig. 1.

The three-phase inverter represents one of the primary sources of electrical noise due to its high-frequency switching operation. Switching strategies such as Pulse Width Modulation (PWM), sinusoidal modulation, and space vector modulation are employed to convert the DC supply from the battery into three-phase AC currents required for motor torque production. However, the rapid switching transitions generate high-frequency voltage and current fluctuations, which introduce unwanted electromagnetic disturbances into the system.

A major portion of this interference is classified as Differential Mode (DM) noise. DM noise flows between the positive and negative high-voltage conductors (HV+ and HV−) within the normal power transmission loop. It is mainly associated with switching ripple currents and voltage oscillations generated by the inverter during operation. Since this noise circulates directly through the power conductors supplying the motor, it can contribute to voltage ripple, additional losses, reduced power quality, and electromagnetic interference within the propulsion system.

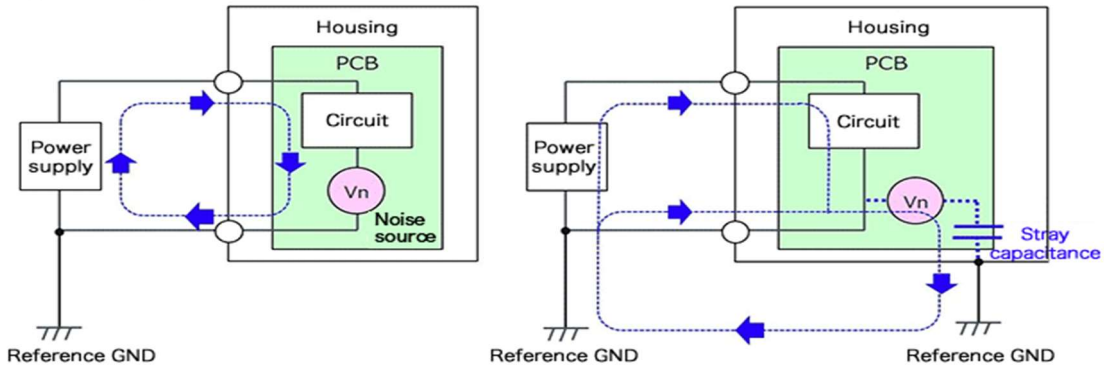

Figure 1. Differential Mode noise and Common Mode noise in EV Propulsion System.

CM noise is another challenge in systems that convert DC to AC, as it results from the switching processes. One set of switches (IGBTs or MOSFETs) is connected to the drain of a second set, which can generate substantial amounts of CM noise when the polarity of the current is reversed. A key mitigation strategy for this CM noise, which also contributes to shaft voltage and bearing currents, is the addition of a CM filter along the motor windings [12]. In conjunction with this, suitable grounding techniques and the implementation of optimal shielded cables can substantially assist in mitigating this issue.

In electric vehicles, common mode (CM) noise is the term used to describe high-frequency current that traverses the high voltage power lines and their return path in the same direction and phase with respect to the chassis ground. This noise is typically transmitted through parasitic capacitance between the vehicle body and cables.

CM noise is impacted by the rate of switching of the power electronic converter which creates rapid voltage or current changes. These changes induce noise through parasitic capacitances. The power module switching behavior and internal parasitic elements influence the magnitude of the CM noise. Therefore, the switching characteristics of the power module is one of the most critical factors in determining its magnitude, which involves device turn-on and turn-off characteristics. The power module parasitic model is essential for understanding the behavior of the power electronics that drive noise generation [12].

Differential Mode noise is characterized by the flow of current in the high voltage power and return lines that are of equal magnitude but in the opposite direction. This form of noise directly impacts line voltage or current, thereby disrupting the operation of power electronics components, including inverters and converters. The propagation of CM and DM noise

throughout the entire Electric Drive System is illustrated in Fig. 2. The concept of CM and DM remains consistent, despite the fact that an actual application may contain multiple modules in the system.

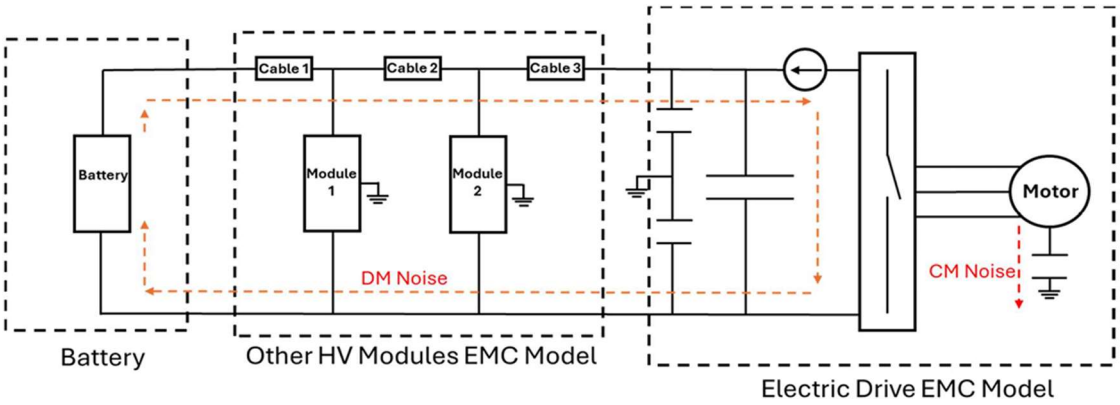

Figure 2. Differential Mode noise and Common Mode noise area in EV System[12].

2.1.2 COMMON MODE CONDUCTED AND RADIATED EMISSION

In battery electric vehicles (BEVs), radiated and conducted emissions are significant electromagnetic compatibility (EMC) issues. The principal source of conducted electromagnetic interference (EMI) in electric vehicles is the inverter, which employs high-frequency switching transistors such as IGBTs or MOSFETs to transform DC power from the battery into AC power for the motor. [12] stated that while this fast switching reduces the size of components and minimizes current ripples and noise, it also leads to rapid voltage and current changes, generating conducted EMI that travels through the vehicle's power cables and can be picked up by other systems. [22] iterated that the high voltages/currents and the fast-switching speeds of inverters in the powertrain can create a hostile electromagnetic environment for other low-voltage systems and passengers via conducted and radiated emissions.

Conducted emissions are referred to as a EMI that travels through the vehicles' wiring and powerlines, and according to [12] it is generally generated by the rapid switching of the power electronics. Conducted emissions interference causes issues with connected components in the vehicle. The DC power bus, AC power bus, cables, wires, or traces are all examples of conducting paths. Conductive emissions from the inverters are transmitted to the battery and motor via DC power bus cables and AC power bus cables. [14] further explains that this conducted EMI couples with electronic circuits in the form of crosstalk and interferes with signal interconnects. The digital signal systems utilized in vehicular electronics architecture typically use isolation between high and low voltage domains.

On the other hand [12], made the distinction of the Radiated emissions that are electromagnetic waves emitted into the surrounding environment from the vehicle's electrical components. Radiated emissions refer to electromagnetic energy that propagates through the air, potentially interfering with other systems.

As the strength of the EMI field in electric vehicles increases, the severity of the electromagnetic compatibility issues also increases. Regulating radiated and conducted emissions is crucial for the reliability, efficiency, and safety of Electric vehicles. By

understanding the origins and by managing the nature of these emissions and employing suitable mitigation strategies, as engineer, can guarantee that the Electric vehicles comply with EMC regulations and operate as designed. Effective noise suppression in electric vehicles can be achieved using filters and chokes.

2.2 DESIGN OF THE FILTER

The design procedure of an electromagnetic interference (EMI) filter can generally be divided into two main stages: the active filter stage and the passive filter stage.
However, in this project, a passive filter is used as it is characterized by its simple design and low cost, demonstrates good performance at low frequencies and currently serves as the primary solution for addressing EMI issues.
As stated by [29] considers not only the filtering performance of PEFs but also practical costs, and PEFs designs and component selections that meet users' requirements.
The overall design of the filter configuration is primarily intended for the suppression of Common Mode (CM) emissions. CM noise, which propagates between the power conductors and the chassis or reference ground, is a major source of conducted and radiated electromagnetic interference in high-frequency power electronic systems such as electric vehicle propulsion systems [2].

2.2.1 DESIGN CONFIGURATION OF THE PASSIVE STAGE FILTER

According to [20] in the explanation of the passive stage filter iterated on the basic components of the Passive stage filters, the basic configuration of a passive filter is shown in Figure 6, where the CM inductor (Lcm), DM inductor (Lcm), X-capacitors (CX1 and Cx2), and Y-capacitor (Cy), respectively. The LCM, also known as a CM choke, consists of two symmetrical wounds on a magnetic core. When CM current flows through it, the magnetic fluxes in the core add up, resulting in a significant inductance that suppresses the CM current. Conversely, when DM current flows, the magnetic fluxes cancel each other out, resulting in negligible inductance, thus allowing the DM current to pass through without attenuation. Consequently, the CM inductor can effectively suppress CM interference in balanced lines without affecting the normally transmitted DM signals. The LDM and CX, CY form a low-pass filter, primarily filtering out differential-mode interference. Simultaneously, the LCM, part of the LDM, and CY also form a low-pass filter, primarily filtering out common-mode interference

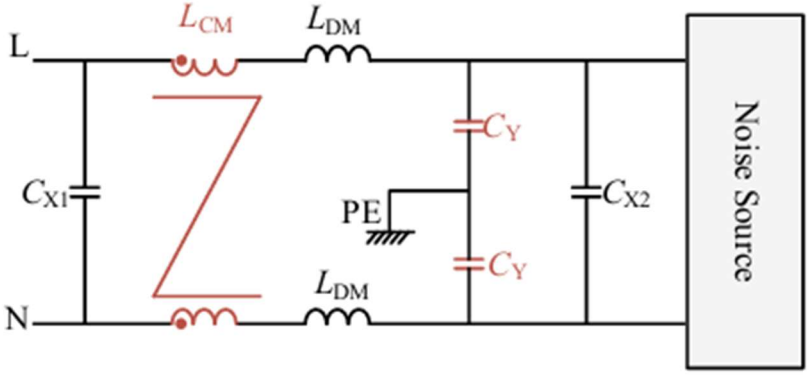

Figure 3. Basic components of Passive Stage Filters [20].

The cutoff frequency is also derived from the expression of the CM and DM noise below using the formulae (1) and (2).

$$f_{c_CM} = \frac{1}{2\pi\sqrt{2C_Y\left(L_{CM} + \frac{1}{2}L_{DM}\right)}} \quad (1)$$

$$f_{c_DM} = \frac{1}{2\pi\sqrt{2C_{X2}L_{DM}}} \quad (2)$$

According to [28] the general approach to passive filter design involves determining the filter's cutoff frequency.
Here, [20] summarizes the design approach for a passive filter into the following aspects

a. Obtain the electromagnetic interference spectrum of the equipment through measurement or prediction, including both DM and CM interference.
b. Select an appropriate filter topology.
c. Determine the filters cut off frequency.

2.3 CONDUCTED ELECTROMAGNETIC INTERFERENCE

Conducted EMI refers to electromagnetic disturbances that propagate through conductive paths such as power cables and electrical connections. It is typically measured in the frequency range from a few kilohertz to tens of megahertz and is a major concern in power electronic systems [18].
Conducted EMI can be categorized into:

- Low-frequency (low-band) EMI: Typically associated with switching harmonics and converter operation
- High-frequency EMI: Associated with fast switching transients and parasitic effects

In grid-to-truck electric powertrain systems, low-band conducted EMI is particularly important because it directly affects power quality and system stability.
A conducted EMI prediction and mitigation strategy that is based on transfer function for the high-low voltage DC-DC converter in EVs are proposed [15].
According to [18], conducted a complete test for the DC-DC converter is conducted to obtain the conducted EMI from DC power cables in the frequency band of 150 kHz-108 MHz.
The test concluded that voltage in frequency range from 150 kHz to 108 MHz can be mitigated to below the limit level 3 of CISPR25 standard (GB/T 18655-2010) by adding the CM interference filters. The DC-DC converter with the CM filter has better stable characteristics and can achieve a good mitigation conducted EMI effect

As stated by [13] Low-band EMI filters are intended to reduce the level of low-frequency conducted emissions that are produced by power electronic switching. These filters are especially crucial in electric vehicle systems, where the EMI spectrum is dominated by switching harmonics.
Inductors are employed to prevent high-frequency currents, while capacitors offer low-impedance pathways for noise signals. CM noise components are frequently suppressed by common-modechokes.
Furthermore, [13] The effective suppression of noise is contingent upon the proper placement of the filter between the EMI source and the remainder of the system.

2.4 Y-Capacitor FOR Common-mode Noise Mitigation

With the rise in switching speed and power density, the electromagnetic interference (EMI) challenges associated with power converters are becoming increasingly severe. Despite the widespread utilization of passive EMI filters (PEFs) in engineering due to their efficacy, their cumbersome components, such as chokes and Y capacitors, impede the improvement of power density in power converters [15].

As further explained by [15] Electromagnetic interference (EMI) concerns, resulting from the rapid switching actions of power electronic converters, affect both the converters and adjacent equipment. As power density escalates, these issues intensify. The predominant method for EMI suppression presently is passive EMI filters (PEFs), which generally consist of components such as common-mode (CM) chokes, Y capacitors are engineered according to the noise source and load impedances.

However, the size of CM chokes is often large due to limitations on Y-capacitors imposed by leakage current safety regulations, posing challenges to the miniaturization and integration of PEFs [15].

Here, [15] states that Y-capacitor primarily increases the effective capacitance value in the frequency range above 1kHz, while maintaining the capacitance values at low frequencies.

A line impedance stabilization network (LISN) is utilized for measuring common mode noise, as mandated by the EMI standard (i.e., CISPR-32), and to mitigate potential external interference from the power supply. Consequently, the common-mode impedance observed from the power supply perspective, in conjunction with the LISN, is comparatively low [16].

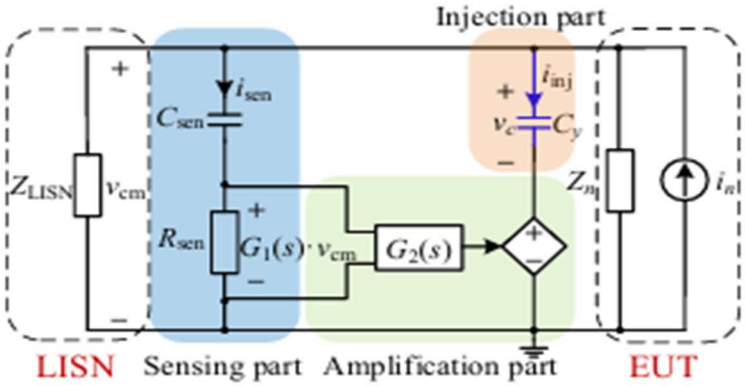

Figure 4. Simplified circuit model of the Y-capacitor [15]

The equivalent circuit of the active Y-capacitor is depicted in Fig. 4. The operational principle and impedance variations of the active Y-capacitor can be illustrated by modeling the amplifier circuit as a regulated voltage source, with G1(s) and G2(s) denoting the transfer functions of the sensing and amplification components, respectively.

2.5 EMC STANDARDS RELATED TO ELECTRIC VEHICLE POWERTRAINS

Automotive EMC standards were established during an era when the primary concern regarding radio-frequency noise from vehicles was the disruption of broadcast transmissions caused by electromagnetic emissions from spark ignition, as vehicle systems were largely mechanical with minimal immunity issues [14]. Continuous technological advancements have altered the characteristics of vehicle emissions and radio-based services at risk, alongside the

increasing implementation of electronic sensors, actuators, and control systems that must operate effectively within a progressively intricate electromagnetic environment.

2.5.1 ELECTRIC VEHICLE EMISSION FREQUENCY RANGE

As noted by [22], the specified frequency range for the emissions measurements outlined in 2004/104/EC, UNECE Regulation 10, and CISPR 12 is between 30 MHz to 1 GHz. [23] states that nonetheless, lower frequencies are recognized to be produced by electric powertrains.

With Increasing deployment of alternative powertrain technologies (e.g. battery, hybrid and fuel cell vehicles) prompted amendments in the 5th Edition of CISPR 12 [7], which is referenced by 2004/104/EC [6].

According to [22] 7th Edition of CISPR 12 that it is necessary that further clarification of conducted and radiated emission measurements for vehicles with electric powertrains.

According to [23] observed that radiated emissions from road vehicles with electric powertrains under acceleration and deceleration conditions may differ from those observed in steady-state dynamic modes (i.e. at constant speed). However, there would be significant practical difficulties in making reliable measurements under such conditions, and conventional vehicles would also need to be tested in a similar manner. The American Society of Automotive Engineers (SAE) Recommended Practice J551-5 specifies the measurement methods and target levels for electric vehicles in the 150 kHz to 30 MHz frequency range. The lower frequency limit was 9 kHz in previous versions; however, it has been raised to 150 kHz to 108MHz in order to comply with CISPR 25.

However, CISPR 25 makes it clear that the voltage method alone is not sufficient to characterize the complete emissions from the device under test (DUT).

3 METHOD

This chapter outlines the methods utilized for conducting research on electromagnetic compatibility modeling and low-frequency electromagnetic interference filter design for grid-to-truck electric powertrain systems utilizing MATLAB/Simulink. The methodology defines the methodologies, instruments, modeling techniques, simulation processes, and analytical methods employed to examine electromagnetic interference (EMI) generation within the electric powertrain system and to devise a suitable low-band EMI filter for the reduction of emissions.

The study employed a simulation-based methodology due to the intricate switching behavior, parasitic interactions, and high-frequency noise propagation associated with electromagnetic compatibility (EMC) analysis in electric vehicle systems, which are challenging and costly to assess experimentally in the initial design phase. MATLAB/Simulink were chosen as the principal simulation platforms because of their proficiency in modeling power electronic converters, control systems, electrical networks, and electromagnetic interference-related phenomena.

3.1 Methodology

This research employed a quantitative simulation-based approach to analyze conducted EMI within a grid-to-truck electric powertrain system. The methodology was carried out in several stages beginning with literature review and system analysis, followed by simulation modeling, EMI analysis, filter design, and performance evaluation.

The overall methodology consisted of the following stages:

1. Information Gathering which includes; Literature/Theoretical study and Powertrain analysis.
2. Model Building which includes; Develop MATLAB/Simulink model, Identify EMIs, EMI analysis of unfiltered system, Design/Integrate EMI filters.
3. Simulate/Evaluate Results; Simulation and Performance evaluation, Analysis of results.

3.2 Model Reduction and Scope of the Simulation

The physical grid-to-truck powertrain consists of several interconnected systems, including the pantograph, grid interface, power conversion stages, DC-link, motor controller, electric motor, and mechanical load. Developing a complete EMC model of the entire system would require detailed modelling of the grid-side converter, pantograph interface, cables, grounding paths, parasitic capacitances and inductances, as well as other electrical components in the vehicle.

However, developing such a detailed model is beyond the scope of this study. Therefore, a reduced electrical model is used for the investigation. In this model, the DC-link supplies the machine-side converter, while the main EMI analysis focuses on the converter output and the electrical network connected to the motor.

The machine-side converter is considered the main source of disturbance because its PWM switching operation generates the voltage and current frequency components investigated in

this study. The filter is placed between the converter and the asynchronous machine to investigate how it affects these switching-related components.
The reduced model does not represent the complete EMC behaviour of the physical grid-to-truck system. Instead, it focuses on an important part of the system: the generation of switching-related disturbances by the motor controller and their propagation towards the traction motor. The results from this simplified model can provide a basis for future work, where the pantograph, grid interface, cable impedance, grounding paths, and other parasitic effects can be included to develop a more complete grid-to-truck EMC model.

3.3 System Design And Simulation

From figure 5; The powertrain model comprises a DC-link supply, a machine-side power electronic converter, a field-oriented control system, voltage and current measurement blocks, a three-stage passive filtering network, an asynchronous machine, and a mechanical load subsystem. The model was created to explore the propagation of converter-generated electrical disturbances via the machine-side electrical network and to assess the impact of passive filtering on the voltage and current spectrum.
From an EMC standpoint, the model can be analyzed using the source-coupling path-victim framework. The machine-side converter is the primary source of disturbance, the three-phase interconnection and filter network comprise the main propagation path, and the asynchronous machine serves as the primary reception subsystem.

3.3.1 DC-Link Supply

The DC-link subsystem supplies the electrical energy needed by the machine-side converter. In the designed model, the DC supply is linked to the converter via the DC-link network.
According to [12] references the DC-link's principal duty is to maintain the DC-side electrical supply necessary for inverter functioning. The DC-link is also essential in terms of EMC since the converter's switching currents can propagate to the DC source. The electrical properties of the DC-link thereby influence the propagation of converter-generated disturbances.
In a practical electric powertrain, the DC-link typically includes capacitive devices designed to reduce DC-bus voltage ripples and provide a local source of switching current for the inverter. The DC-link impedance can interact with the converter and the linked electrical network, especially when parasitic inductances and capacitances are present.
The main EMI study in the current model takes place on the converter's machine side. As a result, the DC-link is generally depicted as an electrical supply subsystem rather than the principal site of conducted emission measurement.

3.3.2 Machine Side Converter

The machine-side converter is the model's main power electronic switching subsystem. It converts the DC-link voltage into the controlled three-phase AC power required to run the asynchronous machine.
The field-oriented control system generates gate signals, which control the converter. The converter generates the appropriate three-phase output voltage via semiconductor switching.
In terms of EMC, the machine-side converter is recognized as the primary disturbance source in the constructed model. The quick switching activity of power electronic equipment generates time-varying voltage and current waveforms. The corresponding voltage and current transition rates are generally expressed as dv/dt and di/dt.

The machine-side converter is shown as a three-phase voltage source inverter (VSI), which transforms the DC power from the DC-link into the three-phase AC voltages necessary for the induction motor. The inverter functions using high-frequency switching devices regulated by PWM gating signals produced by the FOC controller. PWM operation facilitates precise motor control and elevated conversion efficiency; however, the quick switching transitions generate high-frequency voltage and current harmonics within the system. [14] states that the switching events produce both Differential Mode (DM) and Common Mode (CM) noise components, which can disseminate through the propulsion system and contribute to electromagnetic interference.

3.3.3 Field Oriented Control System

The induction-machine field-oriented control subsystem generates the converter gate commands needed to govern machine operation. The control system is given the reference magnetizing current, reference speed, measured three-phase current, rotor-speed data, and DC-link voltage.

In the developed model, the reference magnetizing current is set to 0.7 p.u. at 0.4 s, and the reference speed is set to 1600 rpm at the same time. These reference quantities define the electric machine's operating conditions.

The FOC operates using the per-unit (p.u.) system, where electrical quantities are normalized with respect to predefined base values. The per-unit value is expressed as

$$x_{pu} = \frac{x}{x_{base}} \tag{1}$$

where x = the actual electrical quantity, x_{base} = corresponding base value.

In the developed model, the base current is

$$I_{base} = 296.91 \text{ A}.$$

Therefore, the reference magnetizing current is specified as **0.**7 p.u which corresponds to

$$I_{mr,\text{ref}} = 0.7 \times 296.91 = 207.84 \text{ A}.$$

The field-oriented controller processes feedback signals and creates switching commands for the machine-side converter.

Although the field-oriented controller is not responsible for electromagnetic filtering, it directly influences the generation of conducted electromagnetic interference. The controller determines the converter switching sequence and PWM timing, which establishes the harmonic content of the converter output voltage and current. Consequently, switching frequency, modulation strategy, control-loop dynamics, and operating conditions all contribute to the frequency components observed in the conducted EMI spectra analyzed in Chapter 4.

3.3.4 Voltage and Current Measurement Subsystem

A three-phase voltage and current measurement block is located at the converter's output before the major filter stages.

The measurement subsystem generates the voltage and current signals utilized in analysis. These signals are sent to the appropriate Spectrum Analyzer blocks, allowing the frequency-domain behavior of electrical values to be examined.

The position of the measurement block is critical to the interpretation of the results. The observed signals indicate electrical behavior at the chosen observation point in the converter-

filter-machine network. The Spectrum Analyzer translates time-domain signals to estimated power spectra. The obtained spectrum values are given in dBm based on the analyzer configuration. As a result, the plots are used in this thesis to compare unfiltered and filtered configurations rather than direct standardized EMC receiver readings.

3.3.5 Three Phase Series Inductor / Low-Pass Filter Stage

The first passive filter section consists of a three-phase series inductive stage. Each phase uses an inductance of 21.6 mH. The main purpose of this inductive element is to provide a low-impedance path for the fundamental motor current while increasing the impedance seen by higher-frequency switching components.

The impedance of an ideal inductor is given by:

$$Z_L = \quad \mathrm{j}\omega\mathrm{L}$$

and its magnitude is:

$$| Z_L | \quad = \quad 2\pi f L$$

This shows that the impedance of the inductor increases with frequency. Therefore, the inductive element allows the lower-frequency components required for motor operation to pass while providing increasing opposition to the higher-frequency components generated by the PWM switching.

The inductance of 21.6 mH is retained from the original simulation model. The 21.6 mH inductance is retained in the revised filter configuration, and the filter analysis focuses on its low-pass behavior in the investigated 2–20 kHz frequency range. The filter discussion is therefore focused on the low-pass filtering behavior of the inductive element in the investigated frequency range of 2–20 kHz.

3.3.6 Three Winding Mutual Inductor

The second filter section consists of a three-winding mutual inductor. Each winding has an inductance of

$$L_1 = L_2 = L_3 = 2 \text{ mH},$$

with coupling coefficients

$$k_{12} = k_{13} = k_{23} = 0.9.$$

The high coupling coefficient indicates strong magnetic interaction between the three windings.

The mutual inductance between two coupled windings can be expressed as

$$M = k\sqrt{L_1 L_2}. \tag{4}$$

$$M = 0.9\sqrt{(2 \times 10^{-3})(2 \times 10^{-3})}$$
$$M \approx 1.8 \text{ mH}.$$

3.3.7 Three Phase RC Filter Stage

The final passive filter section is a three-phase RC stage with parameters

$$R = 0.01\ \Omega$$

$$C = 3 \text{ nF}.$$

The RC section is positioned after the coupled-inductor stage and before the asynchronous machine.
The resistor adds a dissipative element to the filter network. The 3 nF capacitive element adds an additional frequency-dependent path to the filter stage. Because capacitive reactance diminishes with increasing frequency, the capacitor's electrical effect increases.
The RC stage should thus be viewed as a dampening and high-frequency shaping component of the proposed multi-stage filter.

3.3.8 Asynchronous Machine

The asynchronous machine illustrates the model's electromechanical energy conversion subsystem. The three-phase electrical amounts provided by the machine-side converter generate electromagnetic torque, which powers the mechanical subsystem.
In terms of EMC, the asynchronous machine is the primary receiving subsystem or victim in the source-path-victim interpretation used in this study.
However, the machine is not electrically passive in the frequency domain. Its stator windings contain resistance and inductance, and the machine structure can cause additional frequency-dependent electrical behavior.

3.3.9 Mechanical Load and Torque Subsystem

The mechanical subsystem applies the load-torque profile to the asynchronous machine.
The model includes a basic torque input and a step-based load-torque command. The mechanical load affects rotor speed and electromagnetic torque demand. Changes in mechanical loading influence the machine's electrical operating condition, affecting the current requested from the converter.
Although the mechanical load is not a direct EMI filtering component, it does affect the electrical operating point at which the spectral analysis is performed.
This relationship is very relevant in electric powertrain EMC studies since converter and machine disturbance behavior varies with operating parameters like speed, torque, modulation index, and load.
As a result, the spectral results provided in this thesis should be evaluated in terms of the precise operating parameters specified in the simulation model.

3.4 Presentation of Results Based on Model and Simulation

This chapter shows the results of the EMI simulations carried out on the full electric vehicle powertrain. It begins with a basic check to confirm that the test setup is correct. After that, the voltage and current spectra are examined to investigate the switching-related conducted disturbances in the model.

3.4.1 Final Simulation Model with Filter

The Simulink/Simscape model represents a Field-Oriented Controlled (FOC) induction motor drive system with a machine-side inverter, EMI-related passive components, sensing blocks, and spectral analysis. This system has been developed and tries to model a grid to truck electric powertrain including filtering and electromagnetic behavior.
For the system level interpretation, the model represents a closed loop induction motor drive with

- Field Oriented Control continuously regulates speed, torque and current

- PWM inverter
- DC-link
- EMI filter structure
- Harmonic analysis
- Induction motor Load

The final simulation model of the grid-to-truck electric powertrain system was created in MATLAB/Simulink with Simscape Electrical components. The model represents the main electrical components of the grid-to-truck powertrain considered in this study, including the DC-link, machine-side converter, switching inverter, filter network, and asynchronous machine. The pantograph, grid-side interface, cable impedance, grounding paths, and other parasitic elements are not included in the current simulation.
The model contains the three-phase converter output passing through the phase inductive elements and then through an additional network before reaching the asynchronous machine. The filtered topology contains a three-phase filtering/interconnection network and a coupled three-phase element before the motor. Therefore, the transfer behavior of the system is influenced by the filter network, machine impedance, phase inductance, and the coupled element.

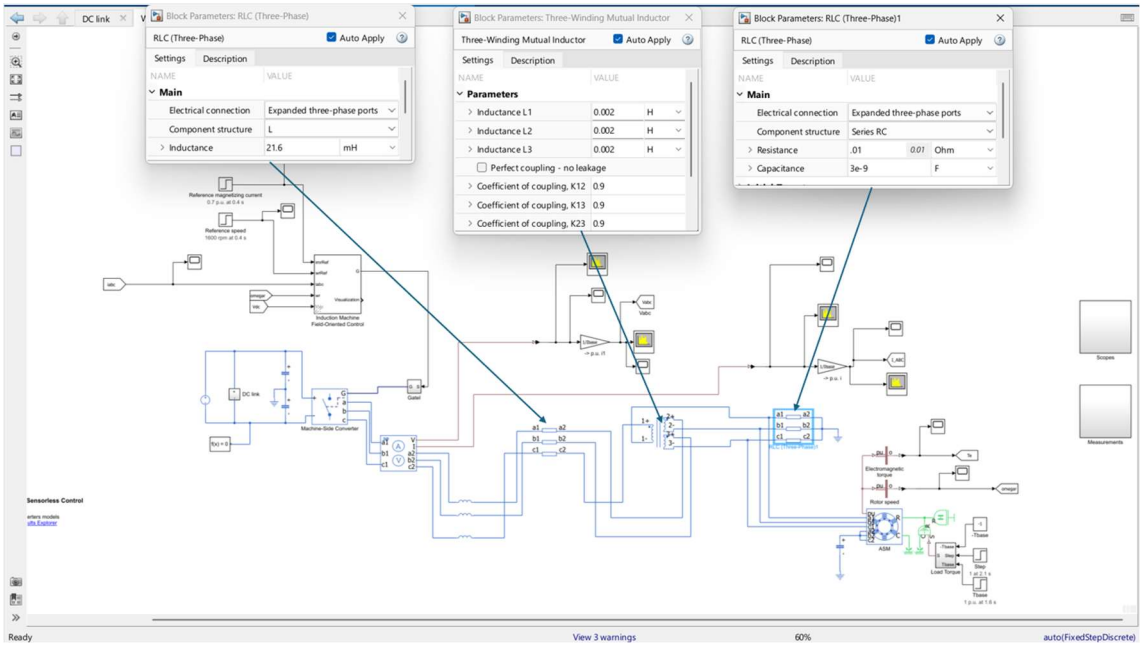

Figure 5. Final Simulation Model with Filter

The filter consists of three passive stages: a series inductor, a coupled inductor, and an RC damping stage. The main purpose of the filter is to reduce the high-frequency components caused by converter switching while allowing the normal motor current to pass through.

Filter Stage	Simulink Configuration	Parameters
1st	Three-phase series inductor	L=21.6mH
2nd	Three-Winding Mutual Inductor	L_1= L_2=L_3=2mH, K_{12}=K_{13}=K_{23}=0.9
3rd	Three-phase RC damping stage	R=0.01 Ohm, C=3nF

Table 1. Simulink Configuration Parameters

The first stage is configured as a three-phase series inductive stage with an inductance of 21.6 mH per phase.The second stage is the three-winding mutual inductor. Each winding has an inductance of 2 mH, and the coupling coefficients are 0.9. A coupling coefficient close to unity indicates strong magnetic coupling between the three windings. The second stage is the three-winding mutual inductor. Each winding has an inductance of 2 mH, and the coupling coefficients are 0.9. A coupling coefficient close to unity indicates strong magnetic coupling between the three windings.
The third stage is a series RC network with $R = 0.01\ \Omega$and $C = 3$ nF.

4 RESULTS

This chapter highlights the simulation outcomes derived from the EMC modeling and low-band EMI filter assessment of the grid-to-truck electric powertrain system utilizing MATLAB/Simulink.
The chapter encompasses the initial examination of the unfiltered system, the determination of conducted EMI characteristics, the implementation of the low-band EMI filter, and a comparative assessment of system performance prior to and following filter integration.
The analysis was carried out with the voltage and current signals obtained from the machine-side electrical measurement step. The signals were analyzed with the Simulink Spectrum Analyzer over a frequency range of about 0-20 kHz. The Spectrum Analyzer conducts frequency-domain spectral estimate and power-spectrum representation in dBm.
The outcomes are examined in three phases. First, the unfiltered and filtered simulation models are compared to determine the EMI source, propagation path, and vulnerable load in the modeled powertrain. Second, voltage and current spectra are examined, with a focus on spectral magnitude, frequency-dependent behavior, local maxima and minima, and residual frequency components. Finally, the two configurations are compared to assess the proposed filter's performance and limits.

Note: The displayed spectrum analyzer quantity is power in dBm.

4.1 CONDUCTED EMI ANALYSIS

4.1.1 EMI SPECTRUM ANALYSIS WITHOUT FILTER

Figure 6 presents the final unfiltered electric powertrain model.
The model consists of a DC-link supply, machine-side converter, three-phase voltage and current measurement stage, phase inductive paths, field-oriented control system, asynchronous machine, and mechanical load subsystem.

The DC-link provides the electrical energy required by the machine-side converter. The converter transforms the DC-link voltage into a controlled three-phase output for operation of the asynchronous machine. The switching operation of the converter represents the principal disturbance-generating mechanism within the modeled system.
The Spectrum Analyzer block in MATLAB/Simulink was used to conduct frequency-domain analysis to determine the spectral distribution of voltage and current disturbances in the system.

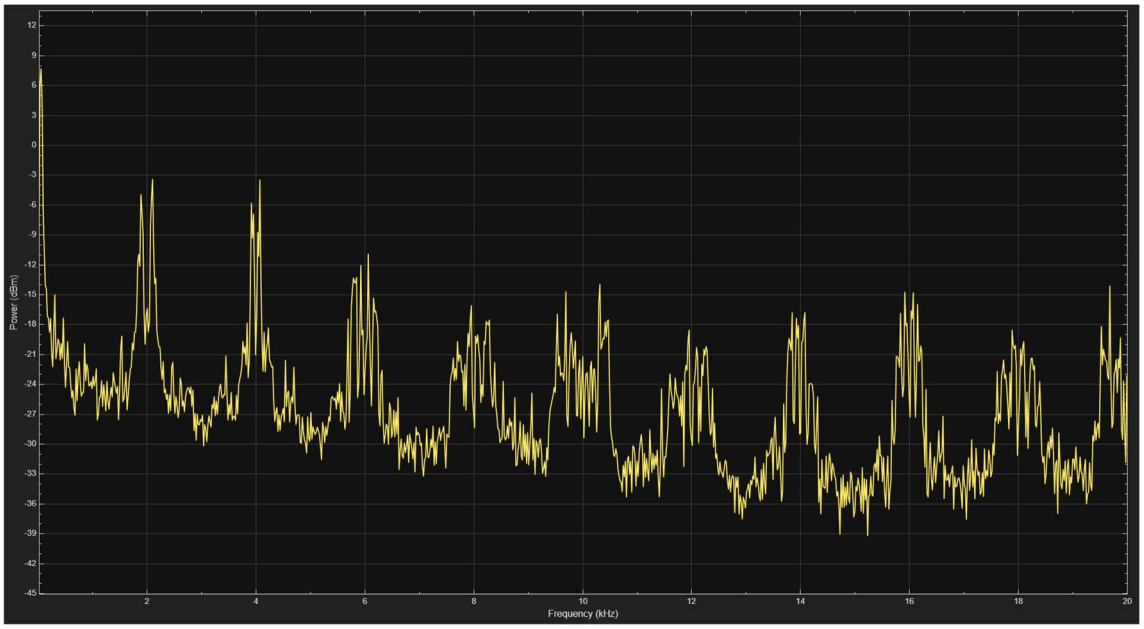

Figure 6. Conducted EMI Voltage Spectrum without EMI Filter

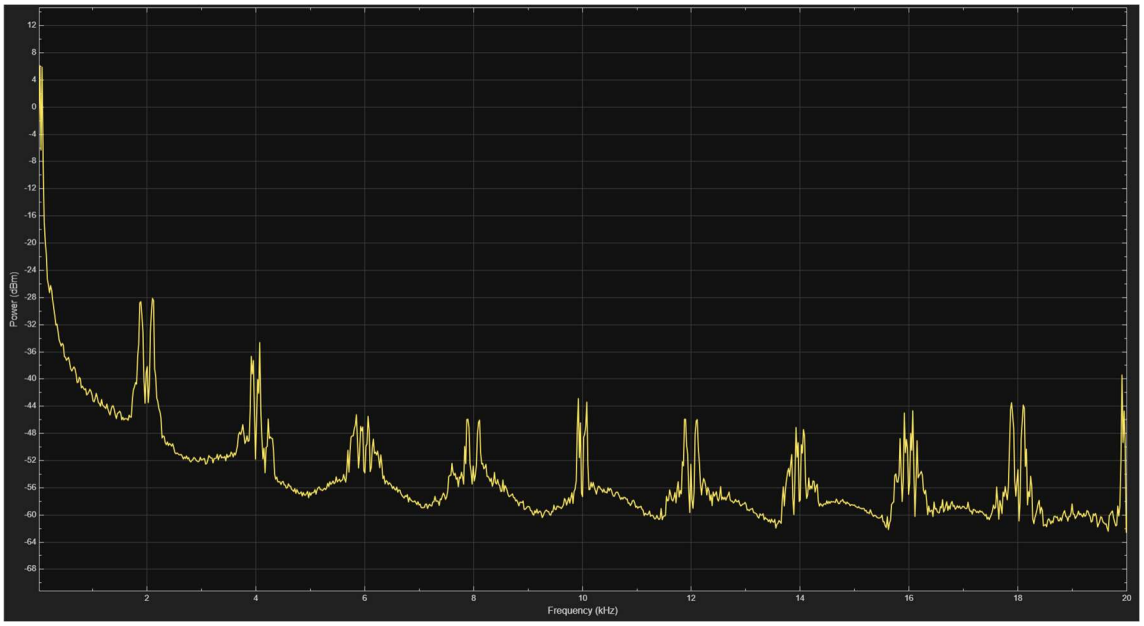

Figure 7. Conducted EMI Current Spectrum without EMI Filter

Figure 6 and 7 The new unfiltered voltage spectrum shows that the inverter switching has a clear influence on the frequency content of the voltage signal. The PWM switching frequency used in the model is 2 kHz, and noticeable peaks can be seen around 2 kHz and at several multiples of this frequency, such as 4, 6, 8, 10 kHz and higher frequencies.

The peaks are stronger in the lower-frequency range and generally become smaller as the frequency increases. However, switching-related components are still visible up to 20 kHz. This pattern is expected in a PWM-controlled inverter, where the switching operation introduces additional frequency components into the output voltage.

A similar pattern can also be seen in the unfiltered current spectrum. Peaks occur at approximately the same frequency intervals, corresponding to the 2 kHz switching frequency and its higher-order harmonics. The overall current spectrum decreases with increasing frequency, although the switching-related peaks remain visible.

These unfiltered voltage and current results are used as the baseline for comparison with the filtered system. By comparing the spectra before and after applying the EMI filter under the same simulation and Spectrum Analyzer settings, the reduction of switching-related frequency components can be evaluated.

Since the Spectrum Analyzer displays the results in dBm, the absolute magnitude depends on the reference and impedance settings used in the analyzer. Therefore, the focus of this study is on the frequency location of the switching components and the relative reduction between the unfiltered and filtered cases, rather than interpreting the displayed dBm values directly as physical EMI power.

4.1.2 EMI SPECTRUM ANALYSIS WITH FILTER

To reduce the conducted disturbances generated by the converter switching, a low-pass EMI filter was placed between the machine-side converter and the induction machine. The main purpose of the filter is to reduce unwanted high-frequency components while maintaining the lower-frequency components required for normal motor operation.

Previous studies have shown that common-mode (CM) and differential-mode (DM) filtering functions can be integrated into the same magnetic component to reduce the size and losses of EMI filters [19]. This can be achieved by introducing additional magnetic paths and windings in a common-mode choke. The resulting leakage inductance can contribute to differential-mode filtering and improve the overall filtering performance [20].

The voltage and current spectra obtained after introducing the EMI filter are shown in Figures 8 and 9. The filtered results were compared with the unfiltered spectra to understand how the filter affects the switching-related frequency components.

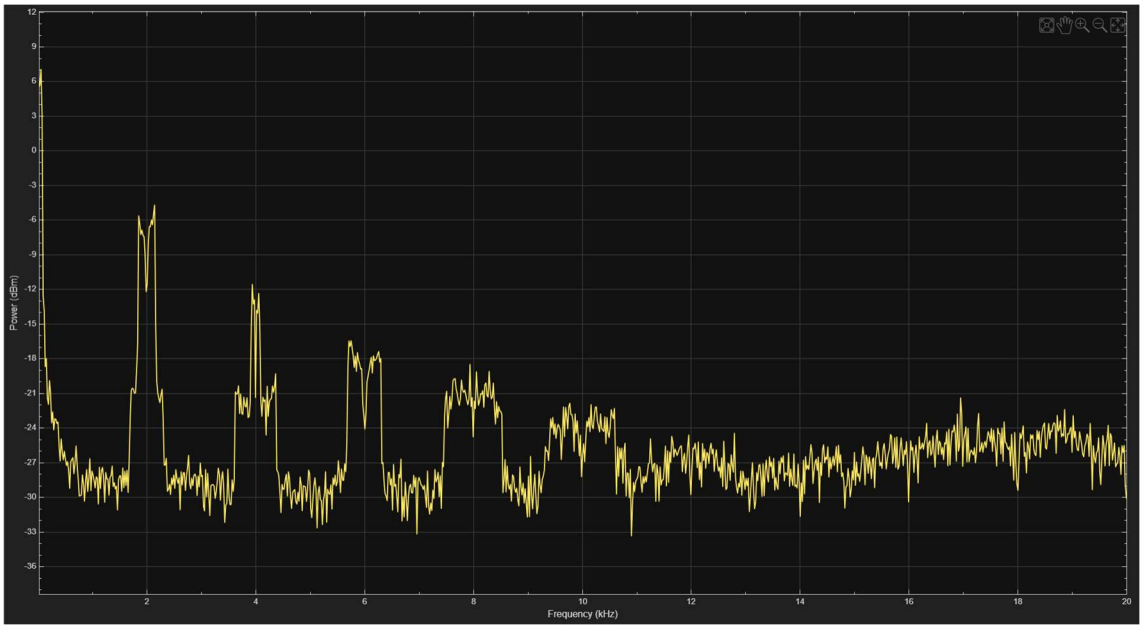

Figure 8. Conducted EMI Voltage Spectrum with EMI Filter

Figure 8 shows the voltage spectrum after introducing the EMI filter. The PWM switching frequency used in the model is 2 kHz, and spectral components can still be observed around the switching frequency and some of its multiples.

A strong component is visible around 2 kHz, followed by smaller components around approximately 4, 6, 8 and 10 kHz. As the frequency increases, the magnitude of these components generally decreases. Above approximately 10 kHz, the individual switching-related components become less dominant, and the spectrum remains mainly around a lower background level.

The filtered spectrum therefore shows that the switching components are not completely removed by the filter. However, their magnitude decreases with increasing frequency, and the higher-order components become considerably less pronounced.

When compared with the unfiltered voltage spectrum, the filtered response shows a reduction in the higher-frequency switching-related content. This indicates that the low-pass filter is reducing part of the high-frequency disturbance generated by the PWM converter while allowing the motor drive to continue operating.

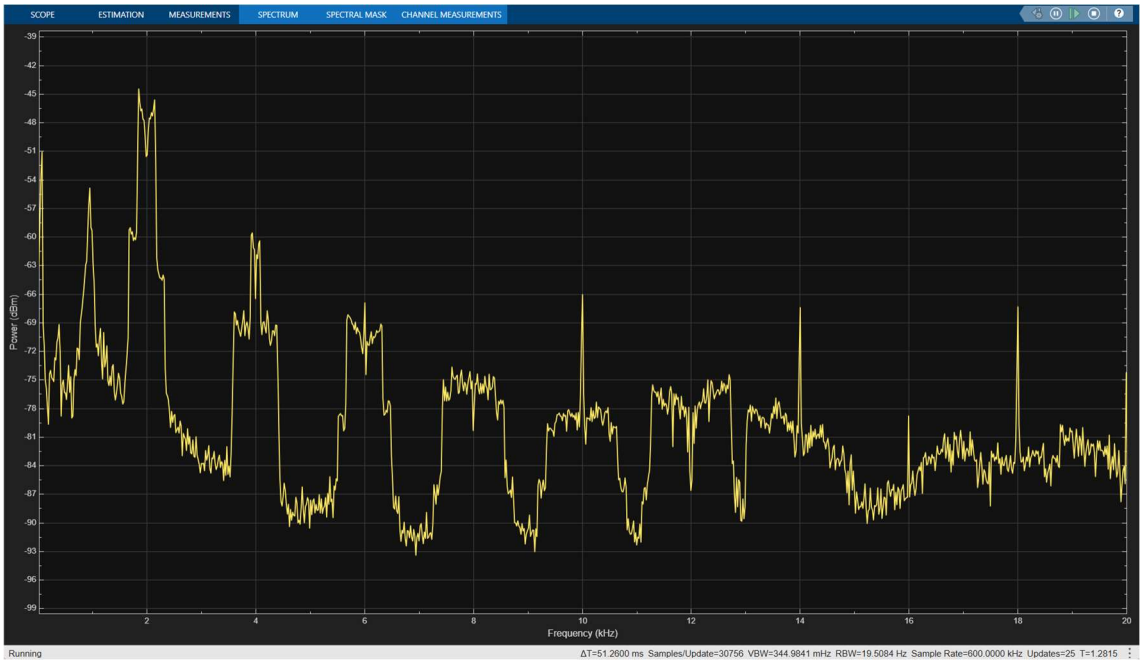

Figure 9. Conducted EMI Current Spectrum with EMI Filter

Figure 9 shows the current spectrum after the introduction of the EMI filter. Similar to the voltage spectrum, the effect of the 2 kHz PWM switching frequency can be observed in the current signal.

The most noticeable switching-related component occurs around 2 kHz. Additional components are visible around 4, 6 and 8 kHz. At higher frequencies, the spectrum generally moves toward lower spectral levels, although some narrow components remain visible around 10, 14 and 18 kHz.

The presence of these remaining peaks shows that the EMI filter does not eliminate all switching-related components. Instead, it reduces their magnitude depending on frequency. This is expected from a practical low-pass filter, where attenuation becomes stronger over certain parts of the frequency range rather than removing all unwanted components completely.

Overall, the filtered current spectrum shows that the higher-order switching components are reduced compared with the dominant lower-frequency components.

Comparison of Unfiltered and Filtered Spectra

The unfiltered voltage and current spectra showed clear components around the 2 kHz switching frequency and its higher-order multiples, including approximately 4, 6, 8 and 10 kHz. These components are mainly related to the PWM switching operation of the machine-side converter.

After introducing the EMI filter, the same switching-frequency pattern can still be identified, but the higher-frequency components become less dominant. This behavior is particularly clear in the voltage spectrum, where the components gradually decrease as frequency increases.

The current spectrum also shows a reduction in the higher-frequency content, although some individual components remain. This means that the filter reduces the switching-related disturbances but does not completely remove them.

The comparison between the unfiltered and filtered cases therefore indicates that the proposed low-pass EMI filter has a clear influence on the frequency content of both the

voltage and current signals. The results support the intended function of the filter, which is to reduce high-frequency switching components while maintaining the normal operation of the electric drive system.
Since the Spectrum Analyzer presents the results in dBm, the absolute magnitude depends on the reference and impedance settings used in the analysis. For this reason, the main focus of the comparison is on the frequency distribution and relative change of the switching-related components before and after filtering, rather than using the displayed dBm values alone to represent absolute conducted EMI power.

4.1.3 Performance Assessment of the EMC

The spectrum analysis gives a clear picture of how the converter switching affects the voltage and current signals in the powertrain system. In the unfiltered results, noticeable frequency components can be seen around the 2 kHz PWM switching frequency and at several multiples of this frequency. This shows that the switching operation of the converter introduces additional high-frequency components into the system.

After introducing the EMI filter, the higher-frequency components are reduced, especially in the voltage spectrum. A similar improvement can also be seen in the current spectrum, although some switching-related components are still present. This is expected, since the purpose of the filter is to reduce unwanted high-frequency disturbances rather than completely remove all frequency components.

The comparison between the filtered and unfiltered results shows that the EMI filter improves the spectral behavior of the simulated powertrain system. The reduction of the higher-frequency components can help improve the EMC performance by limiting the conducted disturbances produced by the converter switching.

The results also support the theoretical concepts discussed in Chapter 3, particularly:

- EMI generation due to power electronic switching
- Common-mode (CM) and differential-mode (DM) noise
- Common-mode choke operation
- EMI filter design
- Y-capacitors for common-mode noise reduction
- The influence of parasitic coupling paths on EMC performance

Overall, the simulation shows that the proposed EMI filter reduces the higher-frequency switching components in the voltage and current spectra. However, some components remain after filtering, showing that there is still room for further adjustment and optimization of the filter design.

5 Discussion of Results

The simulation results show a clear difference between the system before and after the EMI filter was introduced. In the unfiltered condition, several frequency components can be seen around the 2 kHz PWM switching frequency and at multiples of this frequency. These components are mainly related to the switching operation of the inverter.

As discussed in [1] and [2], rapid changes in voltage and current during converter switching are one of the main causes of conducted electromagnetic disturbances. The results from the unfiltered model show similar behavior. This is also in agreement with [3], where inverter switching is identified as an important source of EMI in electric vehicle powertrains. According to [14], the inverter is controlled by PWM signals generated through the field-oriented control system.

After adding the EMI filter, the switching-related components are noticeably reduced. At around 2 kHz, the spectral level decreases from approximately −28 dBm before filtering to −45 dBm after filtering. This gives a reduction of about 17 dB.

A stronger reduction can be seen at some of the higher frequencies. At approximately 4 kHz, the level decreases from −35 dBm to −60 dBm, giving a reduction of about 25 dB. At 6 kHz, the reduction is approximately 23 dB, while at 8 kHz, the level decreases from around −46 dBm to −74 dBm, giving a reduction of approximately 28 dB. At 10 kHz, a reduction of around 23 dB is observed.

Frequency	**Before filter**	**After filter**	**Main observation**
2 kHz	−28 dBm	−45 dBm	Strong reduction
4 kHz	−35 dBm	−60 dBm	Strong reduction
6 kHz	−45 dBm	−68 dBm	Strong reduction
8 kHz	−46 dBm	−74 dBm	Strong reduction
10 kHz	−43 dBm	−66 dBm	Reduced
Higher frequencies	mostly −45 to −60 dBm	mostly −70 to −90 dBm	Noise/spectral level lower

Table 2. Power levels comparison before and after filtering

The comparison shows that the filter has a stronger effect on several of the higher-frequency components. This is the expected behavior of a low-pass filter, since its purpose is to allow the lower-frequency components needed for normal motor operation to pass while reducing unwanted higher-frequency content.

A similar trend can be seen above 10 kHz. Before filtering, much of the spectrum is around −45 to −60 dBm. After filtering, the level is mainly around −70 to −90 dBm. Some individual peaks are still present, but the overall spectral level is lower after the filter is introduced.

The common-mode choke also plays an important role in reducing common-mode disturbances. As discussed in [21], it provides higher impedance to common-mode currents while allowing the normal differential-mode power current to flow with less influence. Together with the inductive and capacitive elements of the filter, this helps to reduce the high-frequency disturbances generated by the inverter.

The filter does not completely remove all the switching-related components. Some peaks are still visible after filtering, particularly around the switching frequency and some of its multiples. This is expected in a practical system because an EMI filter reduces unwanted frequency components rather than completely removing them.

Overall, the results show that the proposed EMI filter reduces the switching-related components over the investigated frequency range. Between 2 and 10 kHz, the reduction is approximately 17–28 dB. The reduction in the higher-frequency content shows that the filter is working as intended and improves the spectral behavior of the simulated powertrain system.

The Spectrum Analyzer presents the results in dBm, and the absolute values depend on the reference and impedance settings used in the analysis. For this reason, the focus of this study is on the relative change between the unfiltered and filtered results obtained using the same simulation and Spectrum Analyzer settings.

The results from the reduced model give an initial understanding of how the switching disturbances from the motor-side converter can be reduced using a passive low-pass filter. The current model does not include the complete pantograph and grid-side electrical system, but the attenuation observed in the 2–20 kHz range provides a useful starting point for further EMC analysis. In future work, the filter can be studied together with a more detailed model of the pantograph, grid impedance, cables, grounding paths, and parasitic elements to better understand its behavior in the complete electrical system.

5.1 Comparison with EMC Standards

The simulation results were considered in relation to CISPR 25:2021 and IEC 61800-3:2022. The comparison is intended to provide EMC context rather than demonstrate regulatory compliance.

Although our study focused on low-band conducted emissions, the findings are comparable to existing EMC norms utilized in electric motor systems and automotive applications.

As outlined by [24] CISPR 25 specifies limits for conducted and radiated emissions in road vehicles within the frequency range of 150 kHz to 108 MHz.

The current simulation analyzes frequencies ranging from 0 to 20 kHz. As a result, there is no frequency overlap between the investigated range and the official CISPR 25 measurement range.

Furthermore, the simulation spectra are expressed as power levels in dBm and were not produced with a typical CISPR measuring arrangement.

As a result, the current findings cannot be directly compared to CISPR 25 emission limitations and cannot be utilized to demonstrate compliance.

Instead, the findings should be characterized as a low-band EMC investigation that falls outside the statutory CISPR 25 measurement range.

The results show that the filter can reduce the switching-related disturbances conducted within the frequency range investigated in this study. However, further modelling and experimental measurements over the relevant EMC frequency range are needed to determine how the filter would perform against formal vehicle EMC requirements.

[26] also stated that in the IEC 61800-3 addresses EMC requirements for adjustable-speed electrical drive systems.

The standard emphasizes: Reduction of common-mode and differential-mode emissions, Proper grounding and shielding, Use of passive EMI filters, Minimization of high-frequency harmonics.
Our simulation results from this study are compatible with these recommendations. The low-pass filter significantly decreases conducted spectrum components while improving overall electromagnetic compatibility.

6 CONCLUSION

This thesis studied electromagnetic compatibility (EMC) and low-band conducted electromagnetic interference (EMI) in a grid-to-truck electric powertrain using MATLAB/Simulink. The main aim was to understand how the switching operation of the power converter affects the voltage and current signals and to investigate how a passive EMI filter can reduce these unwanted frequency components.

The simulation model included the main parts of the electric powertrain, such as the DC-link, machine-side converter, field-oriented control system, three-phase electrical network, asynchronous machine, and mechanical load. The machine-side converter was an important part of the EMC analysis because its PWM switching operation introduces additional high-frequency components into the system.

The voltage and current spectra were first studied without the EMI filter over a frequency range of 0–20 kHz. The PWM switching frequency of the converter was 2 kHz. In the unfiltered results, clear frequency components could be seen around 2 kHz and at several multiples of the switching frequency, including approximately 4, 6, 8 and 10 kHz. This showed the effect of converter switching on the frequency content of the powertrain signals. A three-phase passive EMI filter was then added between the machine-side converter and the asynchronous machine. A three-phase passive EMI filter was then added between the machine-side converter and the asynchronous machine. The revised filter configuration consists of a three-phase series inductive stage with 21.6 mH inductance, a three-winding coupled-inductor stage with 2 mH inductance and a coupling coefficient of 0.9, and a three-phase RC stage with 0.01 Ω resistance and 3 nF capacitances.

After adding the filter, a noticeable reduction could be seen in several of the switching-related components. At approximately 2 kHz, the spectral level decreased from around −28 dBm to −45 dBm, giving a reduction of about 17 dB. At 4 kHz, the reduction was approximately 25 dB. Reductions of around 23 dB at 6 kHz, 28 dB at 8 kHz, and 23 dB at 10 kHz were also observed.

Overall, the selected frequency components between 2 and 10 kHz showed reductions of approximately 17–28 dB after the filter was introduced. The higher-frequency region also generally showed lower spectral levels after filtering. This indicates that the filter is reducing the unwanted higher-frequency content produced by the converter switching.

The filtered results still contain some switching-related components. This is expected because the purpose of the EMI filter is to reduce these components rather than completely remove them. The amount of attenuation also changes with frequency, which is a normal characteristic of a practical low-pass filter.

The Spectrum Analyzer results are presented in dBm. Since the absolute dBm values depend on the reference and impedance settings used in the analysis, the focus of this work is on the relative difference between the unfiltered and filtered results obtained using the same simulation and Spectrum Analyzer settings. Therefore, the results are mainly used to evaluate the performance of the filter within the simulation model.

The frequency range investigated in this thesis was 0–20 kHz. This is below the conventional conducted emission measurement range of CISPR 25, which starts at 150 kHz. For this reason, the results cannot be directly compared with CISPR 25 emission limits or used to demonstrate vehicle-level EMC compliance. The work should instead be considered as a simulation-based study of low-band conducted disturbances and EMI filtering in an electric powertrain.

Overall, the main objective of the thesis was achieved within the scope of the simulation. The electric powertrain model was developed, the switching-related frequency components were identified, and a passive EMI filter was designed and added to the system. By comparing the voltage and current spectra before and after filtering, the effect of the filter could be evaluated. The observed reduction of approximately 17–28 dB at selected frequencies between 2 and 10 kHz shows that the proposed filter can reduce the switching-related high-frequency content in the simulated powertrain.

As for future work, the filter parameters can be further adjusted to improve the reduction of the remaining frequency components. The frequency range can also be extended beyond 20 kHz, together with more detailed cable, parasitic, source, and load models. This would make it possible to study the system under conditions that are closer to practical EMC measurements and relevant automotive EMC standards.

6.1 Limitations of the Work

A notable limitation is the absence of explicit common-mode and differential-mode disturbance separation. Voltage and current measurements were extracted directly from the simulated three-phase electrical network. As a result, the contributions of common-mode and differential-mode disturbances to the measured spectral response were not assessed separately.

Another limitation is related to the frequency range. The current study was limited to a frequency range of around 0-20 kHz. The investigation thus concentrated only on low-band electrical disturbance behavior and did not investigate the higher-frequency conducted-emission spectrum addressed by automobile EMC regulations such as CISPR 25:2021.

Finally, the suggested filter was validated solely using the MATLAB/Simulink simulation environment.

No physical filter prototype, laboratory emission measurement, or hardware-based insertion loss test were carried out.

These limitations do not invalidate comparison simulation results. They do, however, define the range of interpretations for the current study's findings.

The pantograph and the complete grid-side electrical system are not included in the current simulation. Therefore, the results mainly describe the behaviour of the reduced converter–filter–motor system rather than the EMC behaviour of the complete grid-to-truck system.

6.2 Recommendation for Future Work

Future work should use synchronized voltage and current data to calculate the converter-filter-machine system's complicated frequency-dependent impedance. This would allow for a more rigorous investigation of the 16-16.5 kHz interaction, determining if the observed behavior corresponds to real anti-resonance.

The model should be extended to calculate Common Mode and Differential Mode disturbance quantities separately. This would provide a better understanding of the prevailing disturbance mode and allow the filter topology to be tailored for CM, DM, or mixed attenuation.

Future filter models should consider inductor winding resistance, core loss, saturation, inter-winding capacitance, capacitor ESR, capacitor ESL, and frequency-dependent component properties. This would result in a more accurate forecast of practical filter performance.

If further automobile conducted emission comparisons are to be conducted, the frequency range should be expanded to include the formal measurement range of CISPR 25. This would necessitate a faster simulation sample rate and more detailed high-frequency converter and parasitic models.

Future work can build on the reduced model by adding the pantograph, grid-side interface, supply cables, grounding paths, and other relevant parasitic elements. This would make it possible to study the filter in a more complete grid-to-truck system and better understand how disturbances may propagate between the vehicle and the external grid.

References

1. Clayton R. Paul, Introduction to Electromagnetic Compatibility, 2nd Edition, Wiley-Interscience, 2006.
2. Henry W. Ott, Electromagnetic Compatibility Engineering, John Wiley & Sons, 2009.
3. Francesco Profumo, Alessandra Tenconi, and Silvia Vaschetto, "Electromagnetic Compatibility in Electric and Hybrid Vehicles," IEEE Industrial Electronics Magazine, vol. 11, no. 1, pp. 18–27, 2017.
4. V. Khilnani and D. K. Sharma, "EMI Reduction Techniques in Electric Vehicle Power Electronics Systems," International Journal of Power Electronics and Drive Systems, vol. 12, no. 3, pp. 1452–1460, 2021.
5. MathWorks, "Simscape Electrical Documentation," MATLAB/Simulink Documentation. Available:
6. CISPR 25, Vehicles, Boats and Internal Combustion Engines – Radio Disturbance Characteristics – Limits and Methods of Measurement for the Protection of On-board Receivers, International Electrotechnical Commission (IEC), latest edition.
7. ISO 11452, Road Vehicles – Component Test Methods for Electrical Disturbances from Narrowband Radiated Electromagnetic Energy, International Organization for Standardization (ISO).
8. T. Williams, EMC for Product Designers, 5th Edition, Newnes, 2016.
9. C. R. Sullivan and A. Zhang, "Simplified Design Method for Conducted EMI Filters," IEEE Transactions on Power Electronics, vol. 31, no. 10, pp. 7136–7146, 2016.
10. M. H. Rashid, Power Electronics: Circuits, Devices, and Applications, 4th Edition, Pearson Education, 2014.
11. M Anwar, S Bartolucci, S Gleason, M Bellinger, P Leteinturier (2010), "HEV Architectures-Power Electronics Optimization through Collaboration Sub-topic: Inverter Design and Collaboration", SAE Convergence 2010, Detroit, MI.
12. Arash Bavili, Abir Chatterjee, Mohammad Anwar, Brain Gallert, Rebecca Tjoelker, Rahul R*, Nishtha Bajoria*, Yilun Luo, Khorshed Alam Powertrain Design for Noise Mitigation: Addressing EMC/EMI Challenges in Electrified Vehicles
13. Denis Müller1, Konstantin Spanos2, Michael Beltle1, Stefan Tenbohlen, Design of a Hybrid Common - Mode EMI Filter for Traction Inverters in Electrical Vehicles
14. Muthumari P[1]*, Bhuvaneswari S, "Modeling and Analysis of Conducted EMI in a Simulated Electric Vehicle Powertrain" Department of Electrical and Electronics Engineering, S A Engineering College, Chennai, India.
15. Hong Li, Senior Member, IEEE, Siyi Wang, Daozhen He, Zhenyu Zhao, Senior Member, IEEE, Wenzhe Su, Member, IEEE "A Hybrid EMI Filter Incorporating Active Y-capacitor for Common-mode Noise Mitigation".
16. V. Tarateeraseth, K. Y. See, F. G. Canavero and R. W. -Y. Chang, "Systematic Electromagnetic Interference Filter Design Based on Information from In-Circuit Impedance Measurements," IEEE Trans. Electromagn. Compat., vol. 52, no. 3, pp. 588-598, Aug. 2010, doi: 10.1109/TEMC.2010.2046419

17. L. Dai, W. Chen, X. Yang, M. Zheng, Y. Yang and R. Wang, "A Multi-Function Common Mode Choke Based on Active CM EMI Filters for AC/DC Power Converters," IEEE Access, vol. 7, pp. 43534-43546, 2019, doi: 10.1109/ACCESS.2019.2904951.
18. Li Zhai, Tao Zhang, Huiyuan Feng, Yu Cao, Sipeng Yang, Steven Kavuma, "Conducted EMI Prediction and Mitigation Strategy Based on Transfer Function for a High-Low Voltage DC-DC Converter in Electric Vehicle".
19. Rodrigo Drummonda, Bernardo Cougoa, Duc-Hoan Trana, Gregory Almeidaa, Sébastien Serpauda, Victor Dos Santosa, Lenin M.F. Morais "Design optimization of integrated CM/DM inductors for power drive input filter".
20. Chenyu Cao, Panbao Wang, WeiWang and DianguoXu "A Review of Filters for Conducted Electromagnetic Interference Suppression in Converters".
21. T. Erdelyi and T. Van Doren, "Common-Mode Choke Design Considerations for EMI Filters," *IEEE Transactions on Electromagnetic Compatibility*, vol. 54, no. 5, pp. 1156–1163, 2012.
22. Alastair R. Ruddle, and Rob Armstrong, "Review of Current EMC Standards in Relation to Vehicles with Electric Powertrains".
23. A.R. Ruddle, "Investigation of electromagnetic emissions from alternative powertrain road vehicles", MIRA Limited (Nuneaton, UK), Report No. 04-0845060, 28th May 2002.
24. W. H. Hayt, J. A. Buck, Engineering Electromagnetics, 8th ed., McGraw-Hill, New York (2012)
25. MathWorks Inc., Simscape Electrical Documentation, Natick, MA, USA, available at: https://www.mathworks.com/help/physmod/sps/ (accessed October 2025)
26. S. M. L. de Almeida, L. M. de Oliveira, High-frequency modeling of a CISPR 25 LISN for accurate conducted emission prediction, in Proc. IEEE International Symposium on Electromagnetic Compatibility, pp. 1–5 (2021)
27. Y. Li, F. C. Lee, High-frequency modeling of common-mode chokes for automotive EMI filters, IEEE Transactions on Power Electronics, 37 (8), 9105 9118 (2022)
28. Zhang,D,Fan,T.; Ning, P" An Automatic EMI Filter Design Methodology for Electric Vehicle Application. In Proceedings of the 2017 IEEE Energy Conversion Congress and Exposition (ECCE), Cincinnati, OH, USA, 1–5 October 2017; pp. 4497–450
29. Shih, F.-Y.; Chen, D.Y.; Wu, Y.-P.; Chen, Y.-T. A Procedure for Designing EMI Filters for AC Line Applications. IEEE Trans. Power Electron. 1996, 11, 170–18